Optical measurement of micromachine engine performance

Scott C. Holswade and Fred M. Dickey

Sandia National Laboratories
Albuquerque, NM 87185-0328

ABSTRACT

Understanding the mechanisms that impact the performance of Microelectromechanical Systems (MEMS) is essential to the development of optimized designs and drive signals, as well as the qualification of devices for commercial applications. Silicon micromachines include engines that consist of orthogonally oriented linear comb drive actuators mechanically connected to a rotating gear. These gears are as small as 50 μm in diameter and can be driven at rotation rates exceeding 300,000 rpm. Optical techniques offer the potential for measuring long term statistical performance data and transient responses needed to optimize designs and manufacturing techniques. We describe the development of Micromachine Optical Probe (MOP) technology for the evaluation of micromachine performance. The MOP approach is based on the detection of optical signals scattered by the gear teeth or other physical structures. We present experimental results for a prototype system designed to measure engine parameters as well as long term performance data.

Key words: Micromachines, optical probe, performance analysis

1. INTRODUCTION

Microelectromechanical Systems (MEMS), an emerging technology with the potential for revolutionary impact in a wide array of commercial and defense applications, present a unique characterization challenge. The challenge is how to measure the time-dependent spatial position of moving MEMS components, which are on the order of tens of microns in dimension. Such measurements are essential not only to characterize the performance of MEMS actuators, but also to identify and characterize fundamental degradation and failure mechanisms associated with these new types of devices. An infrastructure does not currently exist for easily and fully characterizing micron-sized devices that can move at speeds in excess of 300,000 revolutions per minute.

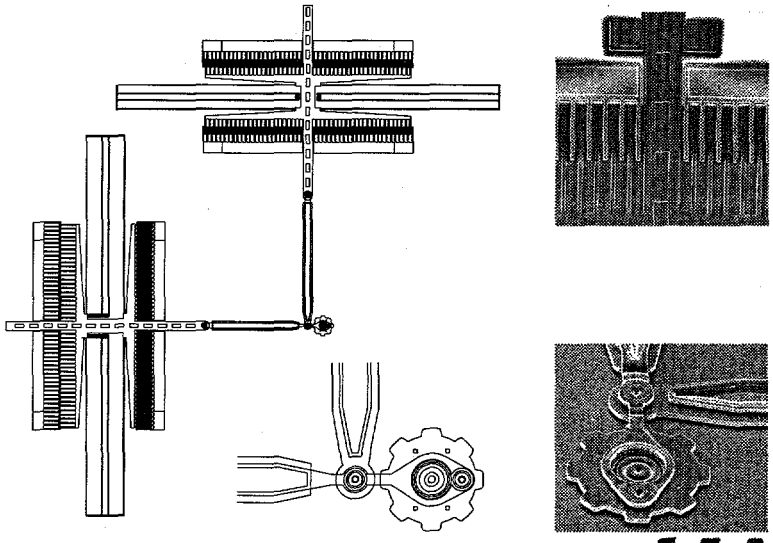

Fig. 1 Microengine diagram.

DISCLAIMER

Consider, for example, the microengine shown in Fig. 1.[1,2,3,4] This devices consists of linear electrostatic actuators that are mechanically coupled to an output gear. Electrostatically applied forces are transmitted to the gear through mechanical linkages in a way that results in continuous rotation of the output gear. The output gear can be used to apply torque to a load device. A description of the technology used to fabricate the microengine is given elsewhere.[1,4] In order to infer fundamental microengine device properties, such as spring constants, electrostatic force constants, and damping coefficients, measurements of the engine response to various applied drive voltages must be made. Time-dependent position measurements of the output gear are also required to measure frictional forces between the gear and hub, and to make performance tradeoffs of the engine in different applications.[5,6] Optimization of the engine drive signals also requires time-dependent position measurements of the output gear. Finally, real-time position measurements are anticipated to be instrumental in identifying fundamental degradation and failure mechanisms associated with the microengine.[7,8]

In the past, position measurements of moving MEMS devices have been made using a strobe light when the engine is driven with periodic signals.[5,6] The strobe technique typically provides images that are the superposition of multiple strobe flashes, resulting in an averaging effect. While this is not a problem when the motion of the device being measured is strictly periodic, non-periodic fluctuations are not able to resolved with the strobe technique. Such fluctuations may be important to understand underlying failure mechanisms of MEMS devices. In addition, automation of the data collection and analysis using the stroboscopic technique requires extensive two-dimensional data processing.

Garcia and Sniegowski[1] used a fiber optic probe to provide evidence that the engine was operating. A method for measuring MEMS device motion has been developed that permits the recording of real-time position information.[9] This method is known as the Micromachine Optical Probe (MOP), and it allows the measurement of non-periodic position fluctuations in the gear. The application of the method consists of measuring light scattered from the gear teeth or other physical structures. In this paper, we present the use of this technique to study engine performance. In the next section we describe the design of the optical probe. Section 3 discusses additional measurement and feedback techniques. We present experimental results for eight and nineteen tooth gear structures in section 4. Finally, section 5 discusses integrated measurement and feedback designs.

2. MICROMACHINE OPTICAL PROBE DESIGN

The Micromachine Optical Probe is based on the simultaneous measurement of forward and back scatter. A schematic of the probe is shown in Fig. 2(a). The source is a HeNe laser which is coupled to a 5 μm core single-mode fiber. Lens L_1 collimates the fiber output and lens L_2 is chosen to give a nominal 3 μm focused spot at the working surface. The backward scattered light collected by L_2 is directed to lens L_3 by the beam splitter and focused on a 1 mm multimode collecting fiber. The forward scatter light is collected by a 1 mm multimode fiber. The axes of the incident (backscatter) and forward scatter beams are coplanar and directed at an angle of 45 degrees with respect to the surface normal. A photograph of the prototype probe installed on a probe station is shown in Fig. 2(b). In the photograph, the forward scatter pickup is on the left and the source backscatter part of the probe is on the right. This configuration of optical signals and detectors is effectively one-dimensional, and it offers the potential of bandwidths in the GHz range. This is sufficient for gears that can be driven at 5 kHz.

Fig. 3 shows a side view of a gear and substrate that are illuminated by the optical probe. Two specular reflections are formed when the outside sections of the incident beam reflect from the substrate and the gear. The side surface of the gear tooth and the substrate form a roof reflector which creates two backscatter reflections from a substrate-to-gear and gear-to-substrate bounce of the incident light. While, this figure shows the conceptual idea of the forward and back scatter beams, the best back scatter signals were obtained with a more complicated reflection geometry.

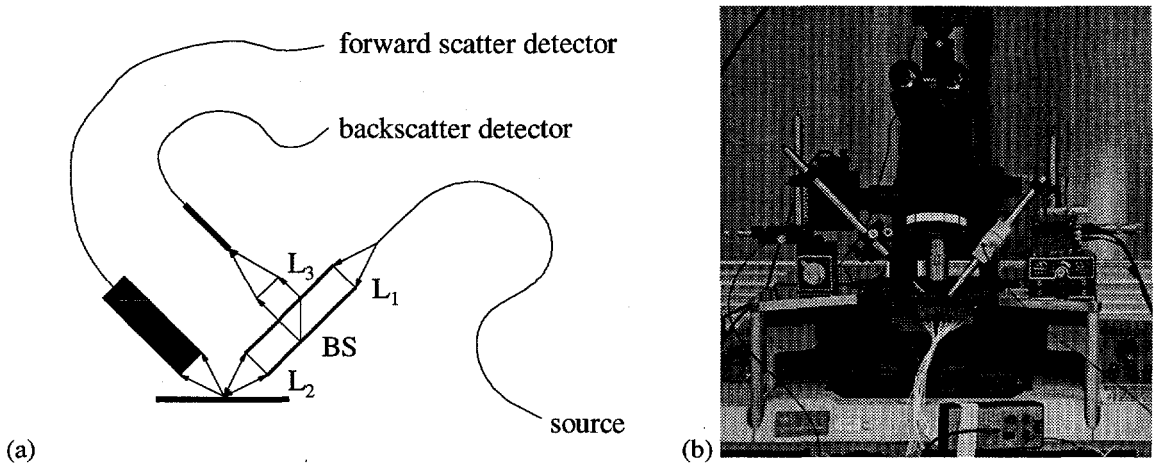

Fig. 2(a) Schematic diagram of the optical probe for forward and backscatter signal detection.
(b) Photograph of probe setup.

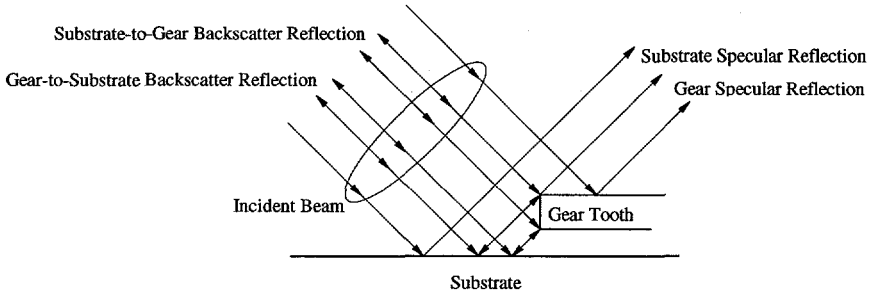

Fig. 3 Forward and backscatter reflected beams created by the geometry of the gear teeth and the substrate below the gear from the incident optical probe beam.

Previous testing of the optical probe established the ability to determine gear speed and direction.[9] It also showed the ability to record non-periodic gear behavior. Finally, it revealed that the back scatter channel provided the best signals for position and speed information. As shown in Fig. 4(a), the best back scatter signals were experimentally observed when the probe beam was incident on the gear at 45° to the tangent. In this case, the incident beam scattered from a corner reflector formed by the substrate, the gear tooth wall, and the inner diameter of the gear. Modeling of the probe has confirmed that the back scatter signal differences depend upon the geometry of the gear teeth rather than any surface scattering behavior.[10] The modeling also investigated the effects of variations in the probe beam size and incident angle.

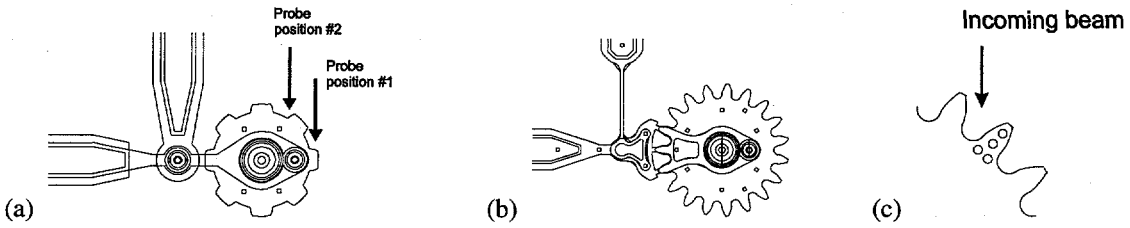

Fig. 4 Gear structures analyzed. (a) Eight-tooth gear. The second incoming probe target point and direction (#2) produced better signals. (b) Nineteen-tooth gear. (c) Example of encoding features added to the nineteen-tooth gear to provide an absolute reference.

A minimum of two signals are needed to sense direction. The optical probe described in this paper uses one source and detects a forward scatter signal and a back scatter signal to obtain direction information. To enhance resolution for some applications, it might be useful to use multiple sensors arranged in a vernier scale. Two sources and detectors, positioned in quadrature phase with respect to a pattern, have been used to make a linear micro encoder.[11]

3. MEASUREMENT AND FEEDBACK TECHNIQUES

Two of the main goals for the probe are the determination of engine device properties and the capture of feedback for the engine drive signals. Measurement of microengine spring and damping parameters can be performed by using a swept frequency approach, as discussed previously.[9] In the following sections, we discuss further issues required to automate measurements, optimize drive signals, and measure additional engine parameters.

3.1. Reference points

While the assessment of engine performance and many of the engine parameters does not require an absolute reference point, there are situations where a reference is advantageous. For example, if the phase delay between the drive signals and the actual engine position needs to be known, a reference point can provide this information. We have encoded a tooth with various features to provide this reference. An example of a reference method is shown in Fig. 4(c). It consists of holes that extend through the gear and provide a back scatter site. At the same time, they reduce the forward scatter from this tooth. This pattern and others are currently in fabrication.

3.2. Friction measurements

A set of equations describing the dynamics of the microengine are needed to develop drive signals and feedback systems. Garcia and Sniegowski[1] derive the general form of the equations of motion using Langrange's equations. Miller et al.[5] derive simplified equations of motion for the microengine shown in Fig. 1. Their equations, which neglect the mass of the gear, are

$$V_x^2 = \frac{1}{\gamma}\frac{k_x r}{a}\left\{\frac{\gamma^2}{\omega_x^2}\left[\left(\ddot{\theta}+2\delta_x\dot{\theta}\right)\cos(\theta)-\dot{\theta}^2\sin(\theta)\right]+\left(\frac{F_r}{k_x r}+\gamma^2\right)\sin(\theta)+\frac{F_l}{k_x r}\cos(\theta)\right\}, \quad (1)$$

$$V_y^2 = \frac{1}{\gamma}\frac{k_y r}{a}\left\{\frac{1}{\omega_x^2}\left[\left(\ddot{\theta}+2\delta_y\dot{\theta}\right)\sin(\theta)+\dot{\theta}^2\cos(\theta)\right]+1-\left(\frac{F_r}{k_y r}+1\right)\cos(\theta)+\frac{F_l}{k_y r}\sin(\theta)\right\}, \quad (2)$$

where k_x and k_y are spring constants, a is the electrostatic force constant relating voltage and applied force, γ is a length ratio related to the drive arms, r is the radius from the gear center to the pin joint, ω_x and ω_y are constants of the form $\sqrt{k/m}$ where k and m are respective spring constants and masses (resonant frequency for small perturbations), and Fr and F_l are the radial and load (tangential) components of the force acting on the gear by the drive arms. For the purposes here, the form of Eqs. (1) and (2) is important, not the details of the constants. Before these equations can be solved for drive voltages, or system dynamics, they must be coupled by an equation relating the forces, F_r and F_l. A first approximation is

$$F_l = \mu F_r, \quad (3)$$

where μ is the friction associated with the gear hub.

Eqs. (1), (2) and (3) can be solved for the drive voltages. For example, the drive voltages for the ideal case of uniform motion and no hub friction can be obtained by substituting

$$\theta = \omega t\,,\; F_l = F_r\,, \tag{4}$$

in the above equations. Once drive voltages are specified, these equations can be used to analyze the response of the microengine. The general equations describing the dynamics of microengines are nonlinear, making the analysis difficult.[1] The above simplified equations as well as the general equations describing electromechanical systems are nonlinear differential equations that are described by a cylindrical or toroidal phase space. For equations of this type there is always the question of stability. Such equations typically have a solution that consists of a linear term plus a periodic function, that is,

$$\theta = \omega t + \phi + p(t/T)\,, \tag{5}$$

where $p(t/T)$ is a periodic function, T is the period of the driving force, and ϕ is a constant phase reference (for fixed drive signals). Ideally, it is desirable to drive the engine so that $p(t/T) = 0$.

The MOP can effectively measure ωt, $p(t/T)$, and changes in ϕ due to changes in drive signals. We believe that this information might be adequate for most control problems and measurement of system parameters. If this is not the case, reference features can be added to measure absolute phase, as discussed in section 3.1. Also, since the probe can measure direction as well as rate, it is possible to keep track of phase if the initial conditions (position) are known.

For purposes of illustration, the response of a microengine like that in Fig. 1 was simulated using DADS® (Dynamic Analysis and Design System) software by DADSI®, Inc. The input drive voltages were obtained using Eqs. (1), (2), and (3). The same values for the system parameters in the equations were also used in the DADS simulation. Fig. 5 is the response of the microengine at frequencies of 305 Hz, 1600 Hz, and 5000 Hz, for a hub friction coefficient of $\mu = 0.4375$. The time axis is in units of periods and each curve is for two cycles. The periodic function is evident in the figure. The first cycle contains transients that decayed by the second and greater cycles.

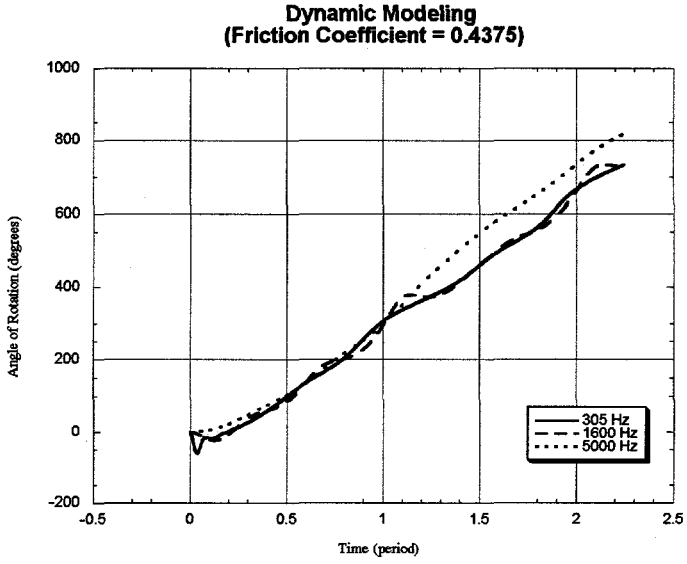

Fig. 5 Modelled engine response for various drive frequencies.

3.3. In-situ drive signal optimization

Currently, experimentally measured engine parameters provide the constants for an equation that produces the engine drive voltages.[5,6] This equation may not be optimum for several reasons: (a) there are significant higher-order terms that were ignored in deriving the equation; (b) the values of the engine parameters contain measurement errors; and (c) a particular engine may contain unique features that cannot be accounted for in the general derivation. There is thus an opportunity to further improve the performance of each particular microengine using optimization guided by performance feedback. A figure of merit, or error function, can be devised that includes such terms as uniformity of rotation, minimum magnitude of applied voltage, and others. The MOP could allow the constants of the drive equation to be modified based on some optimization algorithm, such as damped least squares. Partial derivatives for each drive equation constant could be computed by measuring changes in the error function.

For microengines that are driving other components, load effects will change the dynamic behavior of the system. The drive signals will need to be modified to account for these changing load conditions. Real-time feedback can allow the engine to respond to changing loads and maintain an optimum operating condition. Finally, modeling has suggested that feedback control significantly reduces variation in gear joint forces. This has impact on the long-term wear of the joints and thus engine lifetimes.[1]

3.4. Data reduction

As the experimental data in Section 4 illustrates, the probe detectors produce a signal with peaks that correspond to points where the teeth pass through the beam. For the back scatter case, the peak is formed where the beam returns from the corner reflector formed by the side of the tooth, the inner diameter of the gear, and the substrate. Adequately sampling this signal produces a large amount of data that must be reduced. We have employed a peak detection algorithm to extract the time that each tooth passes by the detector. The back scatter signal provides more precise timing because the corner reflector is only in position for a short time. The back scatter signal is thus the primary measure of performance. The forward signal is broader because it is scattered from the entire width of the tooth. At this time, the forward signal is only used to provide directional information about the gear.

Data reduction begins by locating the forward and back scatter peaks. The phase of the corresponding peaks are compared to provide gear directional information. Assuming that the gear is rotating and not oscillating, the forward scatter information is then discarded. In short, the only information that needs to be stored is the back scatter timing for each of the teeth. This algorithm thus lends itself to real-time data collection and storage, with manageable data sizes.

4. EXPERIMENTAL DATA

The MOP technique's main advantage is that it can provide continuous data for all rotations of the gear. With this information, both uniformity and repeatability of the gear motion can be studied. The following discussion provides and example of the method. For an eight-tooth structure, we collected data for 48 rotations of the gear. Fig. 6 illustrates two back scatter traces from the data set. The uneven spacing of the peaks means that the gear was not sweeping uniformly through its rotation. Peaks four through seven make up half of the gear rotation, yet they occurred in about one-fifth of the total time. This non-uniform movement is largely a result of non-optimized drive signals for this particular gear. Another result from the figure is that the locations of several of the peaks, especially the seventh, have shifted between the two rotations. This means that the motion of the gear differed between the two rotations.

The reasons for the differences in signal amplitude between peaks are still not clear. For the back scatter case, they may be the result of out-of-plane excursions in the gear. These excursions would tend to degrade the corner reflector that forms the back scatter return signal. Variations in both angle and the distance between the gear and the substrate would change the return signal amplitude. Measurement of amplitude uniformity may thus provide an indication of the degree of gear out-of-plane excursions.

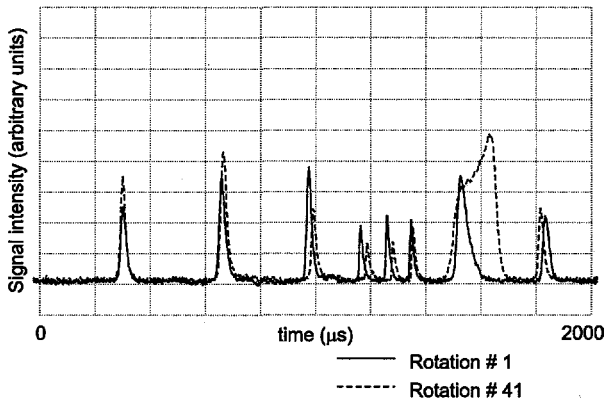

Fig. 6 Back scatter data used to find peak locations. Notice that the position of tooth 7 changes between the two rotations.

After data reduction, the locations of the teeth can be plotted for many rotations, as shown in Fig. 7. The non-uniform rotation of the gear seen in the single traces is evident here. Examination of the figure also reveals the variation in the position of tooth seven as the data were collected. Statistics can be collected for this non-repeatability in tooth position. The data for each tooth can also be fitted to reveal trends in the timing between teeth. This information should prove valuable in the determination of failure precursors. At this time, data collection consists of manually collecting and storing traces on an oscilloscope. The data thus do not show consecutive rotations of the gear. We are currently implementing an automated sampling system that will be capable of continuous data collection and reduction.

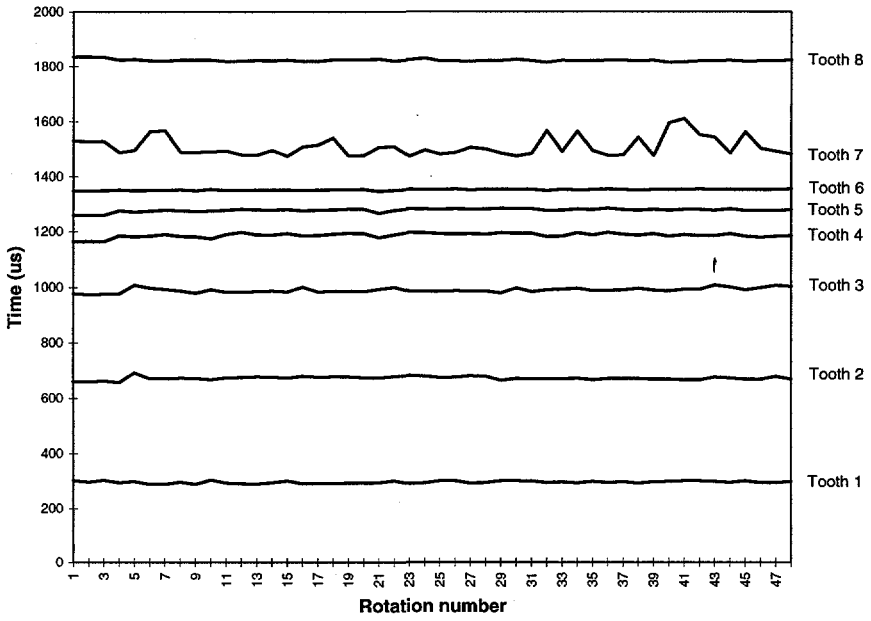

Fig. 7 Gear tooth position versus rotation number. The peak locations illustrated in Fig. 6 are plotted versus rotation number. The rotations are not consecutive.

We have also analyzed the advanced 19-tooth gear structure illustrated in Fig. 4(b). Fig. 8 shows a trace for one rotation, showing peaks for each of the 19 teeth. Again, the uneven spacing of the peaks means that the gear was not sweeping uniformly through its rotation. As shown in Fig. 8(b), the phase difference between the forward and back scatter data determines the rotation direction for this gear.

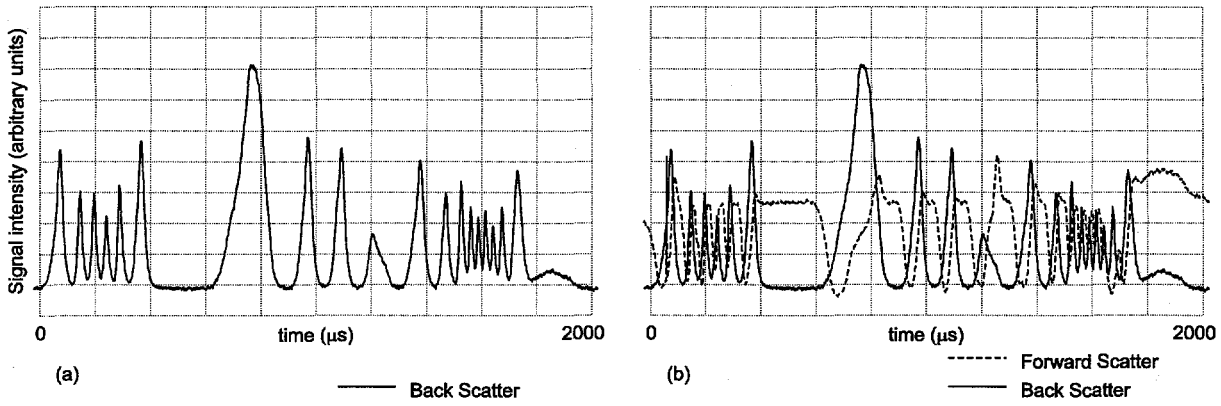

Fig. 8 19-tooth data. (a) Back scatter data only. (b) Both back and forward scatter. One period of the drive signals is shown.

Data for this 19-tooth engine were collected for a series of 25 rotations, as shown in Fig. 9. Non-uniform gear rotation is seen as well as variation in gear motion between rotations.

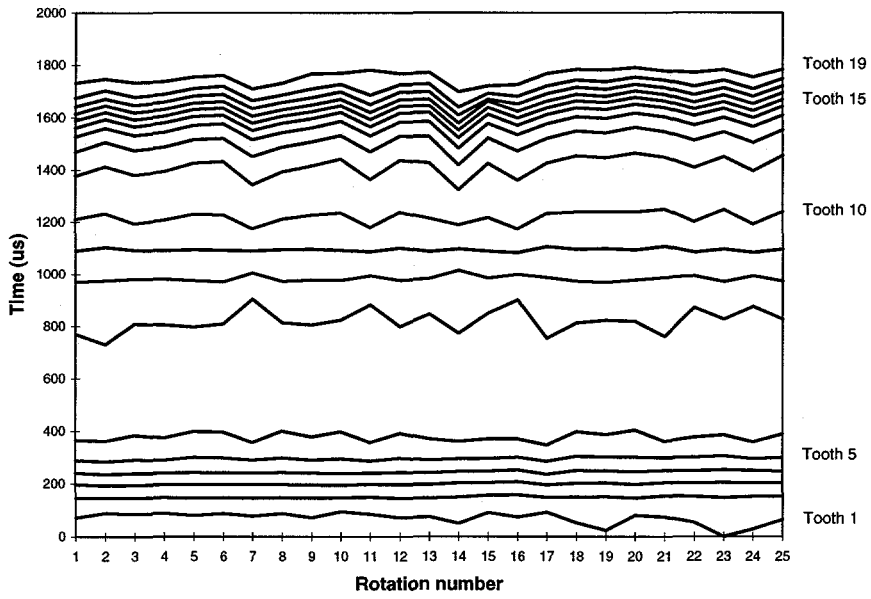

Fig. 9 Gear tooth position versus rotation number. The peak locations illustrated in Fig. 8 are plotted versus rotation number. The rotations are not consecutive.

We also investigated the effects of stopping and starting the gear. Fig. 10(a) shows a trace that is near the end of the same 25 rotation series as Fig. 8 and Fig. 9. The gear was then stopped and restarted. Fig. 10(b) shows a trace taken when the engine was restarted. The traces have similar behavior, except at the last tooth position. For this particular gear, the final tooth position exhibited non-periodic behavior over the complete test series. While more studies need to be done, this preliminary data indicates differences between a stop and restart and no greater than normal non-periodic behavior seen during a continuous operation of the gear. This similarity of behavior after a restart is important for various testing protocols as well as drive signal development.

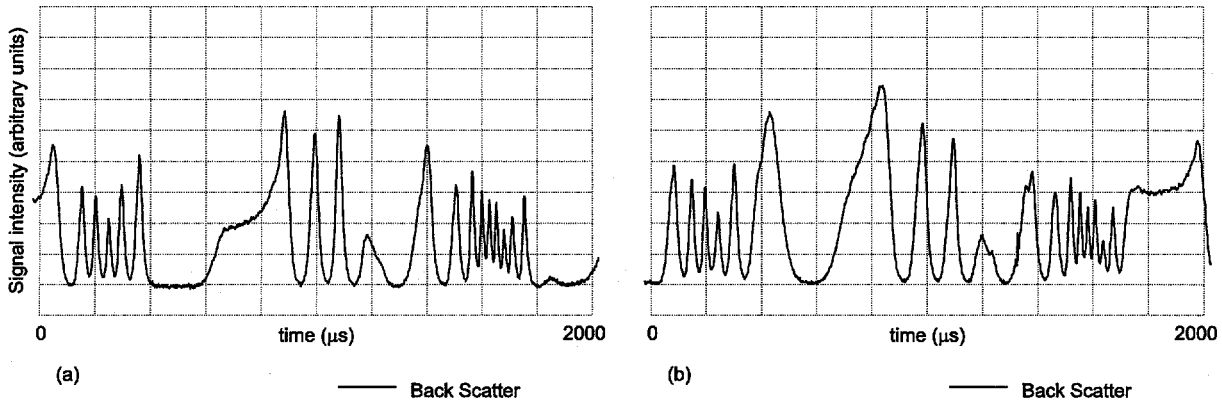

Fig. 10 Results of stopping and starting the engine. (a) Before stopping. (b) After starting again. One period of the drive signals is shown.

5. INTEGRATED OPTICAL FEEDBACK SYSTEMS

Perhaps the most important application of the MOP technology is an integrated feedback system. Besides providing smooth torque output and the ability to respond to changing load conditions, feedback would be important in applications where the state of a mechanical system must be known. Fig. 11 illustrates such a feedback system, with a 19-tooth gear design. In this case, a source fiber or waveguide is positioned close to the gear, with two flanking receiver fibers. An LED or diode laser would provide the source signal. The phase difference between the two receiver fibers would provide direction, and the signal count would record gear motion. Ultimately, the goal is to deposit waveguides during one of the MEMS fabrication steps.

Several technologies may offer a deposition process compatible with MEMS devices. Efforts are underway at Sandia National Laboratories to fabricate polymer waveguides on MEMS devices for optical switching applications. This technology should also enable integrated feedback for MEMS devices. Another technology, microjet printing of micro-optical waveguides, currently can fabricate multimode waveguides on substrates.[12] This technology may be adaptable to the single-mode guides needed for MEMS feedback.

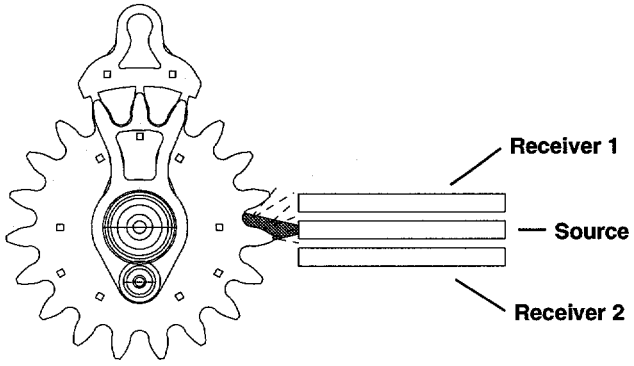

Fig. 11 Integrated feedback system.

6. SUMMARY

In this paper we have presented an optical probe for assessing the performance of silicon micromachines or other actuators for research, development, and applications. A particular configuration of the probe that measures both forward and back scatter was described. Experimental data generated with a prototype optical probe was presented that showed the robustness of the technique. The data demonstrates that the probe generates signals that are adequate for measuring rotation rate, intra-period fluctuations in rotation rate, phase of the rotation relative to the

drive signals and rotation direction of micromachine gears. The quality of the data also suggests that the technique is quite capable of being automated. This technique can also be applied to the detection of motion of other micromachine physical structures.

7. ACKNOWLEDGMENTS

The authors wish to thank T. E. French for developing the peak detection algorithm used to reduce the probe data. They thank E. J. Garcia for portions of Fig. 1 and Fig. 4, T. Mittas for providing Fig. 2(a) and Fig. 3, and G. T. Randall for performing the analysis leading to Fig. 5. This work was supported by the United States Department of Energy under Contract DE-AC04-94AL85000. Sandia is a multiprogram laboratory operated by Sandia Corporation, a Lockheed Martin Company, for the United States Department of Energy.

8. REFERENCES

[1] E. J. Garcia and J. J. Sniegowski, "Surface micromachined microengine", *Sensors and Actuators A*, **48**, pp. 203-214, (1995).

[2] J. J. Sniegowski and E. J. Garcia, "Surface-Micromachined Gear Trains Driven by an On-Chip Electrostatic Microengine", *IEEE Electron Device Lett.*, **17**, pp. 366-368, 1996.

[3] J. J. Sniegowski, S. L. Miller, G. LaVigne, M. S. Rodgers, and P. J. McWhorter, "Monolithic Geared-Mechanisms Driven by a Polysilicon Surface-Micromachined On-chip Electrostatic Engine", *Technical Digest of the 1996 Solid State Sensor and Actuator Workshop*, Hilton Head Island, SC, pp. 178-182, June 3-6, 1996.

[4] J. J. Sniegowski and E. J. Garcia, "Microfabricated actuators and their application to optics", *Proc. SPIE Miniaturized Systems with Micro-Optics and Micromechanics*, Vol. 2383. San Jose, CA, Feb. 7,9, pp. 46-64, 1995.

[5] S. L. Miller, J. J. Sniegowski, G. LaVigne, and P. J. McWhorter, "Friction in Surface Micromachined Microengines", *Proc. SPIE Smart Electronics and MEMS*, Vol. 2722, San Diego, Feb. 28-29, pp. 197-204, 1996.

[6] S. L. Miller, J. J. Sniegowski, G. LaVigne, and P. J. McWhorter, "Performance Tradeoffs for a Surface Micromachined Microengine", *Proc. SPIE Micromachined Devices and Components*, Vol. 2882, Austin, Oct. 14-15, pp. 182-191, 1996.

[7] S. L. Miller, G. LaVigne, M. S. Rodgers, J. J. Sniegowski, and P. J. McWhorter, "Routes to failure in rotating devices experiencing sliding friction", *Proc. SPIE Micromachined Devices and Components*, Vol. 3224, Austin, Sept. 29-30, 1997.

[8] D. M. Tanner, N. F. Smith, D. J. Bowman, W. P. Eaton, and K. A. Peterson, "First Reliability Test of a Surface Micromachined Microengine Using SHiMMeR", *Proc. SPIE Micromachined Devices and Components*, Vol. 3224, Austin, Sept. 29-30, 1997.

[9] F. M. Dickey, S. C. Holswade, N. F. Smith, and S. L. Miller, "An optical probe for micromachine performance analysis", *Proc. SPIE Miniaturized Systems with Micro-Optics and Micromechanics II*, Vol. 3008, San Jose, Feb. 10-12, pp. 52-61, 1997.

[10] A. Mittas, F. M. Dickey, and S. C. Holswade, "Modeling of an optical micromachine probe", *Proc. SPIE Image-Based Motion Measurement II*, Vol. 3173, San Diego, July 27-Aug. 1, 1997.

[11] H. Miyajima, E. Yamamoto, and K. Yanagisawa, "Optical Micro Encoder Using A Twin-Beam VCSEL With Integrated Microlenses," *Transducers '97: International Conference on Solid-State Sensors and Actuators*, Chicago, June 16-19, pp. 1233-1236, 1997.

[12] W. R. Cox, T. Chen, D. J. Hayes, R. F. Hoenigman, and D. L. MacFarlane, "Microjet Printing of Micro-Optical Waveguides", *LEOS '96: Lasers and Electro-Optics Society 9th annual meeting*, Vol. 2, Boston, November, pp. 40-41, 1996.